CORROSION SCIENCE AND TECHNOLOGY, Vol.2, No.4(2003), pp.178~182

Effect of Dissolved Oxygen on the Stress Corrosion Cracking Behavior of 3.5NiCrMoV Steels in High Temperature Water

J. H. Lee, W. Y. Maeng, and U. C. Kim

Nuclear Materials R&D, Korea Atomic Energy Research Institute

Slow Strain Rate Tests (SSRT) were carried out to investigate the effect of environmental factors on the Stress Corrosion Cracking (SCC) susceptibility of 3.5NiCrMoV steels used in discs for Low-Pressure (LP) steam turbines in electric power generating plants. The influences of dissolved oxygen on the stress corrosion cracking of turbine steel were studied. For this purpose, specimens were strained at variously oxygenated conditions at 150℃ in pure water. When the specimen was strained with 1×10^{-7} s^{-1} at 150 ℃ in pure water, increasing concentration of dissolved oxygen decreased the elongation and the UTS. The corrosion potential and the corrosion rate increased as the amounts of dissolved oxygen increased. The increase of the SCC susceptibility of the turbine steel in a highly dissolved oxygen environment is due to the non protectiveness of the oxide layer on the turbine steel surface and the increase of the corrosion current. These results clearly indicate that oxygen concentration increases Stress Corrosion Cracking susceptibility in turbine steel at 150 ℃.

Keywords *: SCC, dissolved oxygen, 3.5NiCrMoV steel, and turbine steel*

1. Introduction

3.5NiCrMoV steel, used as the turbine rotor and disc material of nuclear plants, has experienced various degradation problems such as Stress Corrosion Cracking (SCC), Corrosion Fatigue (CF) and high cycle fatigue. A catastrophic failure of a turbine disc occurred in 1969 at the Hinkley point A nuclear power plant in the United Kingdom.[1] Extensive plant inspections and research programs after the Hinkley Point failure have been conducted worldwide. Cracking was discovered in LP turbine discs of power plants in Australia, South Africa, and the United States.[2)-7)] Disc crackings experienced in these countries were predominantly intergranular, and cracks were normally branched and filled with corrosion products.

According to the analyses of the corrosion products sampled from the failure turbines, it was reported that dissolved oxygen, hydroxide, chloride and sulfate might be the chemical agents causing SCC of LP rotors.[8)] A large number of studies on SCC of rotor materials have been conduced in caustic solutions because of the appearance of hydroxide in the corrosion products of rotors.[4),9)-15)]

There have been severe problems with LP turbine rotors in domestic nuclear plants. In addition to the obvious safety hazard to personnel resulting from such unexpected failure of rotating machinery, the economic cost is enormous. Therefore, the principal objective of this study is to elucidate the influence of dissolved oxygen concentrations on the stress corrosion cracking of LP turbine steels.

2. Experimental Methods

The alloys studied in this investigation have been produced by the DOOSAN Heavy Industries and Construction CO, LTD.

The chemical compositions of the specimens show in Table 1. It met the compositional requirements of ASTM[1)] specifications for A470 materials. Results of tensile test are listed in Table 2.

Table 1. Chemical Composition (wt%) of ASTM A-470 Turbine Disc Steel

Element	ASTM A-470
C	0.24
Si	0.06
Mn	0.30
P	MAX. 0.010
S	MAX. 0.010
Ni	3.5
Cr	1.5
Mo	0.3
V	0.11

1) ASTM, Philadelphia, Pennsylvania.

Table 2. Mechanical Properties of an ASTM A-470 Turbine Disc Steel

Properties	ASTM A-470
Ultimate Tensile Strength(MPa)	785.3
Yield Strength(MPa)	675.1
% Elongation in 25 mm	16

Three liquid water environments were used for the effect of dissolved oxygen on stress corrosion cracking susceptibility. The "de-aerated water" environment contained less than 10 ppb of oxygen. The "intermediate oxygen" environment contained 300-400 ppb of oxygen. The "aerated water" environment was saturated with air, and contained 6-8 ppm of oxygen.

Polarization tests were conducted in the Inconel 625 autoclave with a capacity of 3.78 liters (1 gallon). The specimens were spot-welded to Alloy 600 lead wire which was then covered with a heat shrinkable polytetrafluoroethylene tube for electrical insulation. The specimens were mechanically polished with 2000 grit silicone carbide paper and then ultrasonically cleaned in acetone. The silver-silver chloride (Ag/AgCl) electrode and the platinum plate were used as a reference electrode and counter electrode, respectively.

These polarization tests were carried out using a potentiostat EG&G PAR model 263A. Polarization curves were measured from -0.7 V to 1.4 V at a rate of 0.1 mV/sec.

Specimens[2] for the slow strain rate tests were machined in tensile plate with a 25 mm gage length that had 4 mm × 2 mm (width × thick) dimensions, presented in Fig. 1. The tests were conducted in 3.78 liters (1 gallon) Hastelloy 625 autoclave.

Fig. 2 shows a schematic drawing of the autoclave and the straining fixture constructed so that the tensile action on the specimen is exerted by a downward movement of the crosshead; the speed of the pull rod is moved down 1.5×10^{-4} mm/min by a speed control unit that ensures a constant strain rate during the tests. The equipment used for this purpose was a SERT-C-5000[3].

Elapsed time, applied load, and displacement are recorded at fixed intervals using an external extensometer and by measuring the displacement of the pull road with respect to the autoclave head. Before each experiment, the tensile specimens were degreased in acetone. The autoclave was then filled with high-purity water. While purging with high-purity nitrogen to eliminate the oxygen,

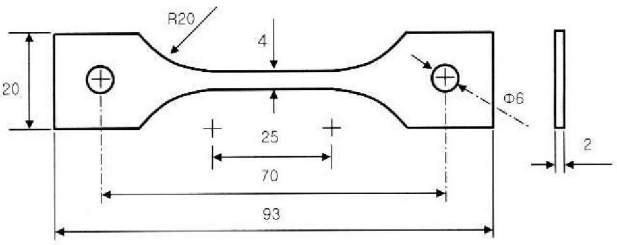

Fig. 1. Geometry of SSRT test specimen (unit: mm).

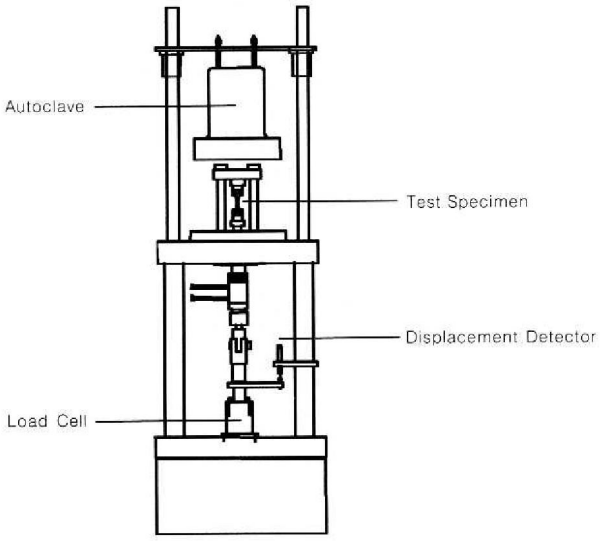

Fig. 2. Schematic drawing of the slow strain rate tester.

the specimens were kept stress free. The tests were performed at a strain rate of 1×10^{-7} s^{-1}.

The load applied to each specimen was recorded at constant intervals as a function of time, and engineering stress vs. time curve was produced for each specimen. Reductions of area (RA) and percent elongation (I%) were determined from measurement of the fractured specimen. In all cases, each specimen was observed under the Scanning Electron Microscope (SEM) to determine the mode of cracking.

3. Results

To examine the effect of dissolved oxygen on the stress corrosion cracking susceptibility, specimens were strained to failure at 150 ℃ in pure water containing various amounts of oxygen and at the strain rate of 1×10^{-7} s^{-1}.

The results are illustrated in Fig. 3 where the stress is presented as a function of elongation. Reduction of area (RA) decreased as dissolved oxygen increased, shown in Fig. 4. Elongation was 14% in a deaerated water environment, and intermediate-oxygen and aerated water environment were 11% and 6 % respectively; elongation de

2) The tensile specimens were tested in the as-ground condition.
3) Manufactured by Toshin Kogyo Co., Ltd.

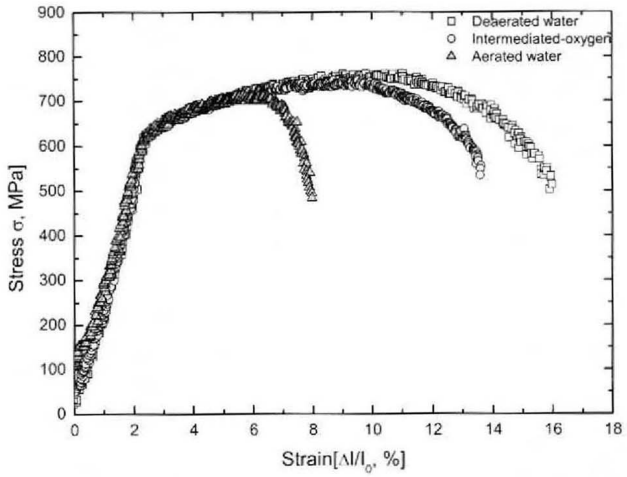

Fig. 3. Stress strain curves produced form data recorded during SSRT test results in varied environments with the strain rate of 10^{-7} s^{-1} at 150℃.

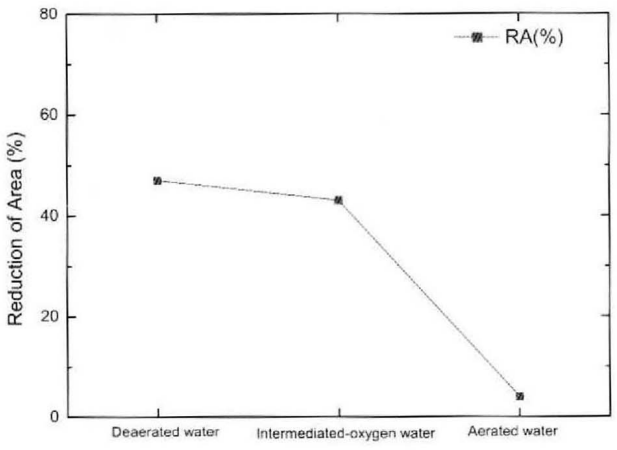

Fig. 4. Reduction area value of SSRT test results in varied environments with the strain rate of 10^{-7} s^{-1} at 150℃.

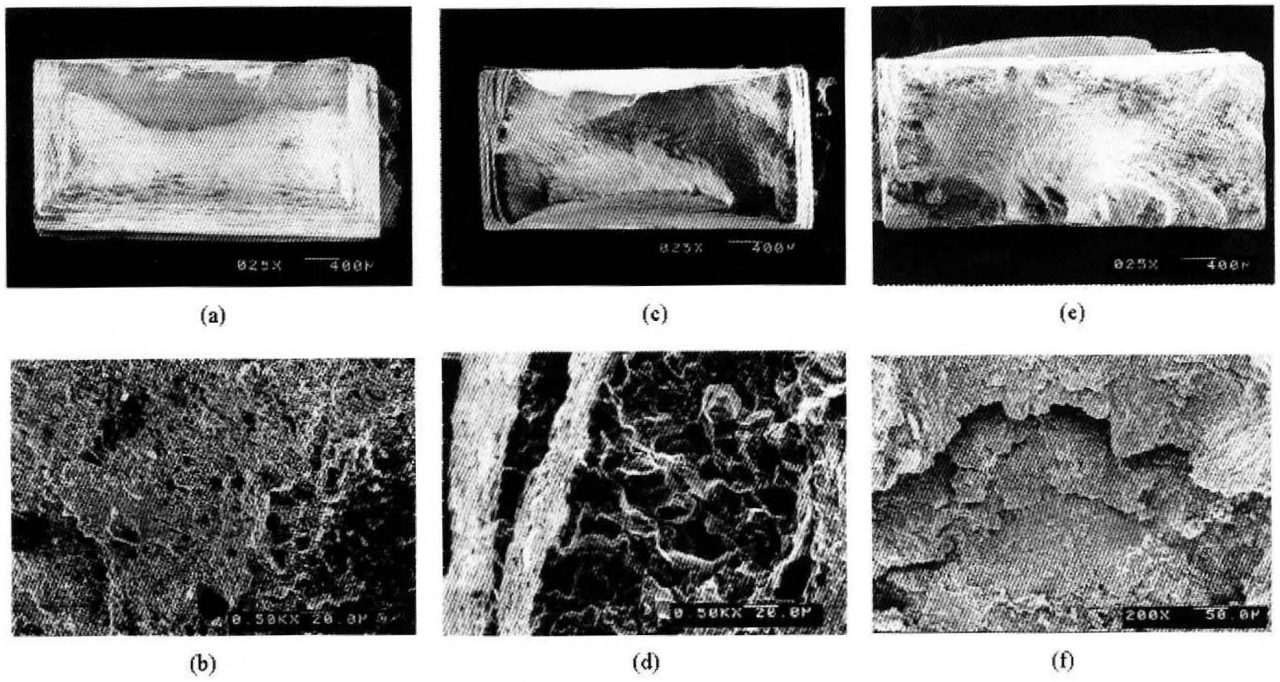

Fig. 5. Fracture surfaces failure in SSRT test at 150℃; (a) Deaerated water - top view, (b) Deaerated water - enlargement showing ductile rupture, (c) Intermediated - top view, (d) Intermediated - enlargement showing IGSCC, (e) Aerated water - top view, (f) Aerated water - enlargement showing IGSCC.

Table 3. Effect of the amount of dissolved oxygen on SCC Test Results at 150℃

	Elongation (%)	UTS (MPa)	RA (%)	Failure time (h)
Aerated water	6	714	4	262
Intermediate-oxygen water	11	745	43	393
Deaerated water	14	761	47	453

creased as dissolved oxygen increased. UTS decreased as dissolved oxygen increased. The values of elongation and UTS of 3.5NiCrMoV steel in various amounts of dissolved oxygen are presented in Table 3.

Under the deaerated experimental conditions, the ductile fracture occurred without any influence from the corrosive medium and exhibited the dimple morphology, shown in Fig. 5 (a) and (b). At intermediate-oxygen conditions, intergranular stress corrosion cracking was exhibited out-

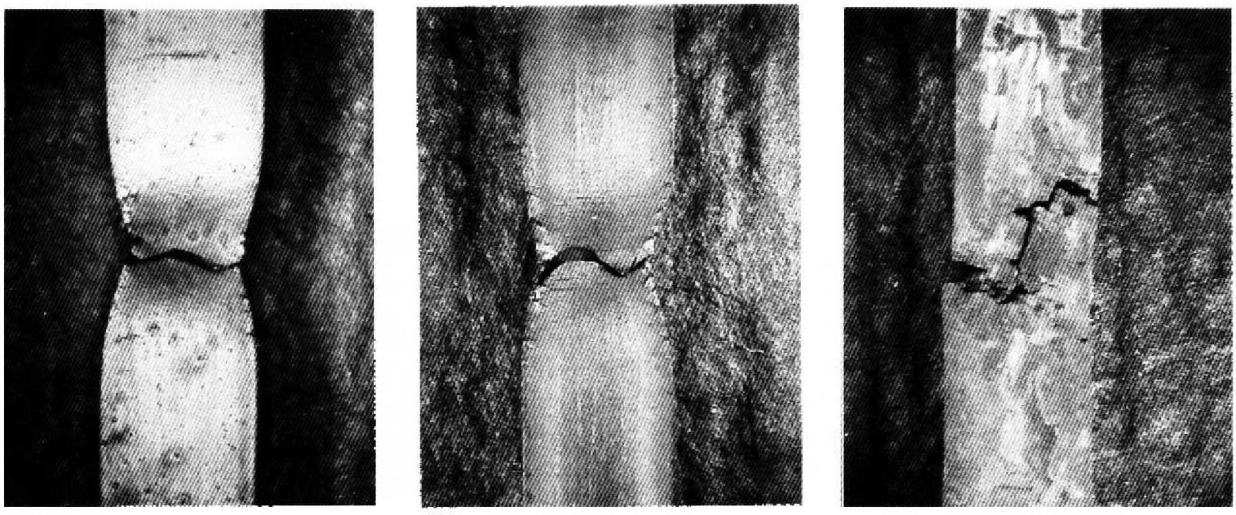

(a) (b) (c)

Fig. 6. Fracture morphologies tested in varied environments with the strain rate of 10^{-7} s^{-1} at 150℃; (a) Deaerated water, (b) Intermediated, (c) Aerated water.

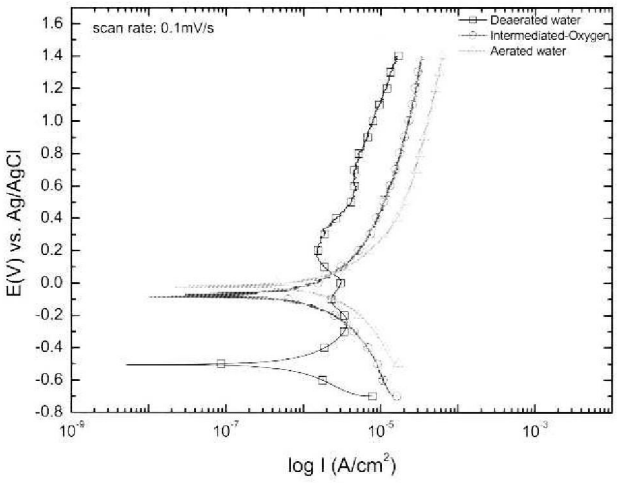

Fig. 7. Polarization curves of 3.5NiCrMoV steel in varied environments at 150℃: scan rate-0.1mV/s.

Table 4. The values of corrosion potential and corrosion current density in varied environments at 150℃

	Corrosion potential (mV)	Corrosion current density (nA/cm²)
Aerated water	-21	1460
Intermediate-oxygen water	-75	772
Deaerated water	-505	420

side the fracture surface. And the final mechanical fracture was ductile, which is shown in the typical dimple morphology. They are indicated in Fig. 5 (c) and (d). Around the intermediate-oxygen condition's fracture surface, like deaerated condition', was a large deformation: which formed a necking. Unlike the deaerated condition's result, however, secondary cracks were shown around the necking, illustrated in Fig. 6. Under the aerated condition, the fracture surface, shown in Fig. 5 (e) and (f), was filled with corrosion products and exhibited stress corrosion cracking.

The polarization curves, tested in varied environments at 150 ℃, are shown in Fig. 7. The corrosion potentials and the corrosion current densities are presented in Table 4. The corrosion potential and the corrosion density all decreased as the amounts of dissolved oxygen decreased.

4. Discussion

Dissolved oxygen, according to the test results of this study, significantly influences the stress corrosion cracking behavior of 3.5NiCrMoV steel. Stress Corrosion Cracking susceptibility of 3.5NiCrMoV steel increased as the amounts of dissolved oxygen increased.

It is considered that the increase of Stress Corrosion Cracking susceptibility has an intimate relation with the increase of corrosion current in the corrosive environment. Corrosion of a metal is accomplished by the combination of oxidation of the metal and reduction of hydrogen ions or oxygen molecules. In the case of a high concentration of dissolved oxygen in water, the reduction reaction in the corrosion process is mainly accomplished by the oxide reduction as in this reaction.[16]

Anodic reaction:

$$M \rightarrow M^{n+} + ne^-$$

Cathodic reaction:

$$O_2 + 2H_2O + 4e^- \rightarrow 4OH^-$$

or

$$2H_2O + 2e^- = H_2 + 2OH^-$$

M is the anodic element dissolved and may be Fe, Ni, Cr or Mo. The cathodic process is reduction of dissolved oxygen. If the concentration of dissolved oxygen in this reduction reaction increases, the current for this reduction increases. The corrosion potential is decided at the point where the total rate of oxidation is equal to the total reduction. So the increase of reduction current increases the oxidation current and consequently increases the corrosion potential in the anodic range of potential if no passive film is formed on the metal. When passive film is formed by the oxidation of corroding metal, the current density in the passive range drastically decreases during the corrosion process. But there is no decreasing range of current density beyond corrosion potential in 3.5NiCrMoV steel as shown in Fig. 7. It is considered that a passive film does not form in the steel. So the corrosion current increases as the corrosion potential increases in the steel because of the highly dissolved oxygen concentration. Increasing dissolved oxygen, therefore, increases the corrosion potential, and then the increasing corrosion potential causes an increase in the corrosion current density.

According to Table 4, actually, the corrosion current density of the 3.5NiCrMoV steel is 420 $nA \cdot cm^{-2}$ in a deaerated water environment while the corrosion current density of the steel is 1460 $nA \cdot cm^{-2}$ in an aerated water environment. The corrosion current and corrosion potential increase as the dissolved oxygen concentration increases. The increase of the corrosion current in the water of higher dissolved oxygen concentration is deeply related with the highly SCC susceptibility of the 3.5NiCrMoV steel in that environment.

5. Conclusions

The dissolved oxygen concentration clearly influences the SCC susceptibility of 3.5NiCrMoV steel at 150 ℃ in pure water. When a specimen was strained with 1×10^{-7} s^{-1} at 150 ℃ in pure water, increasing concentration of dissolved oxygen decreased the elongation and the UTS. The corrosion potential and the corrosion rate all increased as the amounts of dissolved oxygen increased. These results clearly indicate that Stress corrosion cracking susceptibility of 3.5NiCrMoV steel at 150 ℃ increased as the amounts of dissolved oxygen increased.

Acknowledgements

This work has been carried out under the nuclear research and development program of the Ministry of Science and Technology of Korea.

References

1. J. M. Hodge and I. L. Mogford, "U.K Experience of Stress Corrosion Cracking in Steam Turbine Discs", *Proc. Inst. Mech. Eng.*, **193**, 93-109 (1979).
2. Ellery, A. R., Journal of the Australasion Institute of Metals, **21**, 103-111, June-Sept. (1976).
3. Schleithoff, K., Stress Corrosion Cracking in Steam Turbine Components-Sase Histories, Laboratory tests and Service Experience, Paper Presented at EPRI/CERL Workshop on Turbine Disc Cracking at Central Electricity Research Laboratories, Leatherhead, Englan, Nov. 28-30 (1979).
4. McCord, T. G., Bussert, N. W., Curran, R. M., and Gould, G. C., Materials perfomance, **15**(2), 25, February (1976).
5. Lyle, F. F., Jr., Bursle, A. J., Burghard, H. C., Jr., and Leverant, G. R., Stress Corrosion Cracking of Steels in Low-Pressure Turbine Environments, Corrsion/80 (Paper 233), NACE, March 1980.
6. Lindinger, R. J., and Curran, R. M., Experience with Stress Corrosion Cracking in Large Steam Turbines, Corrosion/81 (Paper 7), NACE, April 1981.
7. Lyle, F. F., Jr, and Burghard, H. C., Jr., Identification of Potential Key Variables Responsible for Cracking of Low-Pressure Rotor Discs, EPRI Research Projict 1398-5, Task 1, Phase I and Task 2, Phase I, Final Report
8. O. Jonas, Corrosion/77, San Francisco. California, 14-18 March No. 124 (1977).
9. J. G. Parker, Br. Corros. J. **8**, 124 (1973).
10. R. S. Shalvoy, S. K. Duglin and R. R. Lindinger, Corrosion/81, 6-10 April, Ontario, Canada, No.7 (1881).
11. G. T. Buestein and J. Woodward, Rev. Coat. Corros. **6**(1), 82 (1984).
12. R. S. Shalvoy, "The Effect of Potential and Caustic Concentration on the Stress Corrosion Cracking of NiCrMoV Steel at 100 C", Corr. 39, pp.66~70 (1983).
13. Fred F. Lyle, Jr., "Stress Corrosion Cracking Characterization of 3.5 NiCrMoV Low Pressure Turbine Rotor Steels in NaOH and NaCl Solutions", Corr. **39**, 120~131 (1983).
14. N. Bandyopadhyay and C. L. Briat, "Caustic Stress Corrosion Cracking of NiCrMoV Rotor Steels- The Eddects of Inpurity Segregation and Variation in Alloy Composition", Metall. Trans. A **14A**, 2005-2019 (1983).
15. A. McMinn and F. F. Lyle, EPRI Report, NP3634 (1984).
16. J. Y. Liu and C. C. Su, "Environmental Effects in the Stress Corrosion Cracking of Turbine Disc Steels", Corrosion Science, **36**, 2017-2028 (1994).